J Appl Electrochem (2010) 40:393–399
DOI 10.1007/s10800-009-0009-x

ORIGINAL PAPER

# A study of hydroxyethyl imidazoline as $H_2S$ corrosion inhibitor using electrochemical noise and electrochemical impedance spectroscopy

**M. A. Lucio-Garcia · J. G. Gonzalez-Rodriguez · A. Martinez-Villafañe · G. Dominguez-Patiño · M. A. Neri-Flores · J. G. Chacon-Nava**

Received: 16 October 2008 / Accepted: 1 September 2009 / Published online: 27 September 2009


**Abstract** A study of $H_2S$ corrosion inhibition of pipeline steel by hydroxyethyl imidazoline has been carried out by using electrochemical techniques. Inhibitor concentration included 5, 10, 25, 50, and 100 ppm in a $H_2S$-containing 3% NaCl solution at 50 °C. Techniques included linear polarization resistance (LPR), electrochemical impedance spectroscopy (EIS), and electrochemical noise (EN) measurements. In addition to the traditional noise in voltage and current, noise resistance ($R_n$) measurements were used. All techniques showed that the most efficient inhibitor concentration was between 5 and 10 ppm, but inhibitor efficiency decreased after 8 h of testing. Furthermore, EN measurements showed that steel was highly susceptible to localized corrosion at inhibitor doses lower than 10 ppm due to the establishment of a porous inhibitor film. However, with 50 or 100 ppm of inhibitor, the steel was susceptible to a mixture of uniform and localized corrosion. Hurst exponent was higher in presence of inhibitor for times shorter than 8 h, indicating a short residence time of the inhibitor. The data could not be fitted to any adsorption isotherm model, indicating a lack of strong adsorption of the inhibitor to the metal surface.

**Keywords** Electrochemical noise · Electrochemical impedance · Hydroxyethyl imidazoline · Hurst

M. A. Lucio-Garcia · J. G. Gonzalez-Rodriguez · A. Martinez-Villafañe · M. A. Neri-Flores · J. G. Chacon-Nava
Centro de Investigacion en Materiales Avanzados, S.C.-Miguel de Cervantes 120, Complejo Industrial Chihuahua, Chihuahua, Mexico

J. G. Gonzalez-Rodriguez (✉) · G. Dominguez-Patiño
UAEM-CIICAp, Av. Universidad 1001,
62209 Cuernavaca, Morelos, Mexico
e-mail: ggonzalez@uaem.mx

## 1 Introduction

Oilfield corrosion manifests itself in several forms, where $CO_2$ corrosion (sweet corrosion), hydrogen sulfide ($H_2S$) corrosion (sour corrosion), and corrosion by oxygen dissolved in water injection are by far the most prevalent forms of attack found in oil and gas production [1]. Because of its applications in different industries, corrosion of steel in $H_2S$-containing solutions is a well-known phenomenon that has been investigated for years [2, 3]. Corrosion inhibitor injection is standard practice in oil and gas production systems to control internal corrosion in carbon steel structures. Nitrogen-based organic inhibitors, such as imidazolines or their salts have been successfully used in these applications even without an understanding of the inhibition mechanism [4–6]. Corrosion inhibition of organic compounds is related to the adsorption properties of the organic compounds and depends on the nature and state of the metal surface, type of corrosive environment, and chemical structure of the inhibitor [7–9].

Among the different electrochemical techniques that can be used to evaluate inhibitors, electrochemical impedance spectroscopy (EIS) appears to be a powerful tool due to the information it provides in addition to traditional techniques such as polarization curves or linear polarization resistance (LPR) measurements. Moreover, electrochemical noise (EN) measurements have also been successfully applied to the study of corrosion inhibitors' performance [10–13]. These measurements are made without any external perturbation of the system and provide information of the actual system being studied with little possibility of artifacts due to the measurement technique.

EN technique involves the estimation of the electrochemical noise resistance, $R_n$, which is calculated as the standard deviation of potential, $\sigma_v$, divided by the standard deviation of current, $\sigma_i$,

$$R_n = \sigma_v/\sigma_i \quad (1)$$

where $R_n$ can be taken as the linear polarization resistance, $R_p$ in the Stern–Geary equation:

$$I_{corr} = (b_a b_c)/\left[2.3(b_a + b_c)R_p\right] \quad (2)$$

and thus, inversely proportional to the corrosion rate, $I_{corr}$, but with the necessary condition that trend removal is applied over an average baseline as previously established by Tan et al. [14]. It has been shown that the noise signal contains information about the dynamics that occur on the surface of the electrode and gives information about the type of corrosion that is occurring, either uniform or localized. Thus, the aim of this study is to evaluate the performance of a simple organic compound such as hydroxyethyl imidazoline as a $H_2S$ corrosion inhibitor by comparing results obtained by three different electrochemical techniques such as LPR, EIS, and EN measurements.

## 2 Experimental procedure

### 2.1 Testing material

Material tested was a pipeline with a chemical composition as given in Table 1, with a martensitic microstructure resulting from heating it at 867 °C during 30 min, and then water quenched.

#### *2.1.1 Testing solution*

Inhibitor used in this study was a commercial hydroxyethyl imidazoline with a general structure as shown in Fig. 1. Inhibitor was dissolved in pure 2-propanol. The concentration of the inhibitor used in this study was 0, 5, 10, 25, 50, and 100 ppm, and the temperature was kept at 50 °C. The testing solution consisted of 3 wt% NaCl solution which was heated and deaerated with nitrogen gas. $H_2S$ was produced by reacting 3.53 mg $L^{-1}$ Sodium Sulfide ($Na_2S$) with 1.7 mg $L^{-1}$ Acetic acid. Inhibitor was added 2 h after pre-corroding the specimen with a micro syringe. This is because in practice, inside the pipelines, the corrosive environment is inhibitor free, and it is after some time that the inhibitor is added. Electrochemical measurements were taken 20 min later. All this procedure is recommended in the NACE MR0175-2003 specification [15].

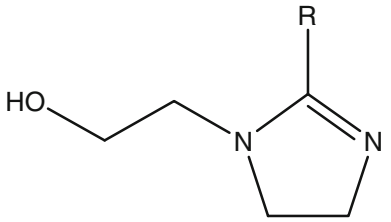


**Fig. 1** General structure of hydroxyethyl imidazoline, where R is an alkyl chain derivative

$H_2S$ concentration was 45 mM which was calculated by using the following equation:

$$2NaCl + Na_2S + 4CH_3COOH \rightarrow 4H_2S + 4CH_3COONa + H_2S + 2HCl \quad (3)$$

### 2.2 Electrochemical measurements

Electrochemical techniques employed included linear polarization resistance, LPR, electrochemical impedance spectroscopy, EIS, and electrochemical noise, EN, measurements, in both current and voltage. Measurements were obtained, each one separately, step by step, by using a conventional three electrode glass cell with two symmetrically distributed graphite counter electrodes and a saturated calomel electrode (SCE) as reference with a Lugging capillary bridge. LPR measurements were carried out by polarizing the specimen from +10 to −10 mV respect to $E_{corr}$, at a scanning rate of 1 mV $s^{-1}$ every 20 min during 24 h. Electrochemical impedance spectroscopy tests were carried out at $E_{corr}$ by using a signal with amplitude of 10 mV and a frequency interval of 0.1 Hz–30 kHz. An ACM potentiostat controlled by a desk top computer was used for the LPR tests, whereas for the EIS measurements, a model PC4 300 Gamry potentiostat was used. Finally, EN measurements in both current and potential were recorded with two identical working electrodes and a reference electrode (SCE). EN measurements were carried out by simultaneously recording the potential and current fluctuations at a sampling rate of 1 point/s for a period of 1024 s. A fully automated zero resistance ammeter (ZRA) from ACM instruments was used in this case. Removal of the DC trend from raw noise data was the first step in the noise analysis when needed. In order to accomplish this, a least square fitting method was used. Finally, the noise resistance, $R_n$, was then calculated as the ratio of the potential noise standard deviation over the current noise standard deviation.

**Table 1** Chemical composition of used steel (wt%)

| C | Si | Mn | P | S | Cr | Ni | Ti | V | Cu | Nb | Mo | Al |
|---|---|---|---|---|---|---|---|---|---|---|---|---|
| 0.044 | 0.271 | 1.69 | 0.009 | 0.001 | 0.010 | 0.240 | 0.014 | 0.001 | 0.217 | 0.055 | 0.25 | 0.0310 |

## 3 Results and discussion

Figure 2 summarizes the LPR results, showing variation of $R_p$ over time for uninhibited and inhibited solutions at all different inhibitor concentrations. Regardless of the inhibitor concentration, even for the solution without inhibitor, $R_p$ decreased with time, indicating an increase in the corrosion rate with elapsed time. In solutions containing $H_2S$, carbon steels corrosion process is generally accompanied by the formation of a sulfide film [16, 17]. The fact that $R_p$ increased first over time and after a while it decreased suggests the non-protective nature of the corrosion products film. The film is a non-adherent layer which can be easily removed from the steel surface and cannot passivate the steel surface under the environmental conditions used here. The protectiveness of the inhibitor film should depend among other factors, on the adherence and stability of the inhibitor on this iron sulfide film.

As soon as the inhibitor was added, $R_p$ increased, and thus, the corrosion rate decreased. $R_p$ reached its highest value by adding 10 ppm inhibitor. For lower or higher inhibitor concentrations, $R_p$ was lower than that obtained with 10 ppm, the concentration that produced the lowest corrosion rate. However, similar to the solutions without inhibitor, the $R_p$ of inhibited solutions decreased over time, showing an increase in the corrosion rate. For exposure times longer than 8 h, the $R_p$ values for solutions without inhibitor were slightly higher than those obtained by adding either 5 or 10 ppm of inhibitor. In general, it has been accepted that inhibitors form a protective layer on the surface of the metal. However, the decrease in the $R_p$ value shows that this film inhibitor was unstable and detached from the metal surface. Furthermore, the metal was left unprotected and exhibited a higher corrosion rate. Thus, the kinetics of the detaching process such as slight desorption or breaking, along with the FeS corrosion products of the inhibitor can be analyzed from $R_p$.

The Nyquist data for the 3% NaCl solution without inhibitor is shown Fig. 3a. The impedance spectra show, in all the cases, a single (capacitive-like) depressed semicircle indicating a process under charge transfer control. In such a process, the semicircle diameter is equivalent to the linear polarization resistance value, $R_p$. It can be seen that semicircle diameter increased with time. This indicates that the corrosion rate was decreasing as time elapsed. However, after 24 h of testing, the semicircle diameter decreased, indicating an increase in the corrosion rate at this time. The Bode diagram in the modulus versus log (frequency) format, Fig. 3b, showed an increase in the modulus with time until 8 h, and a decrease for longer times. When 10 ppm of inhibitor was added (Fig. 4a), two semicircles were observed: one at high frequencies, related

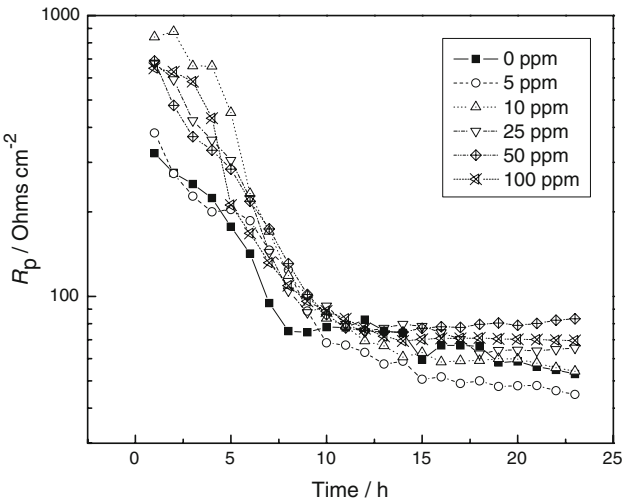


**Fig. 2** Effect of hydroxyethyl imidazoline concentration on the change in $R_p$ over time in $H_2S$-containing 3% NaCl solution

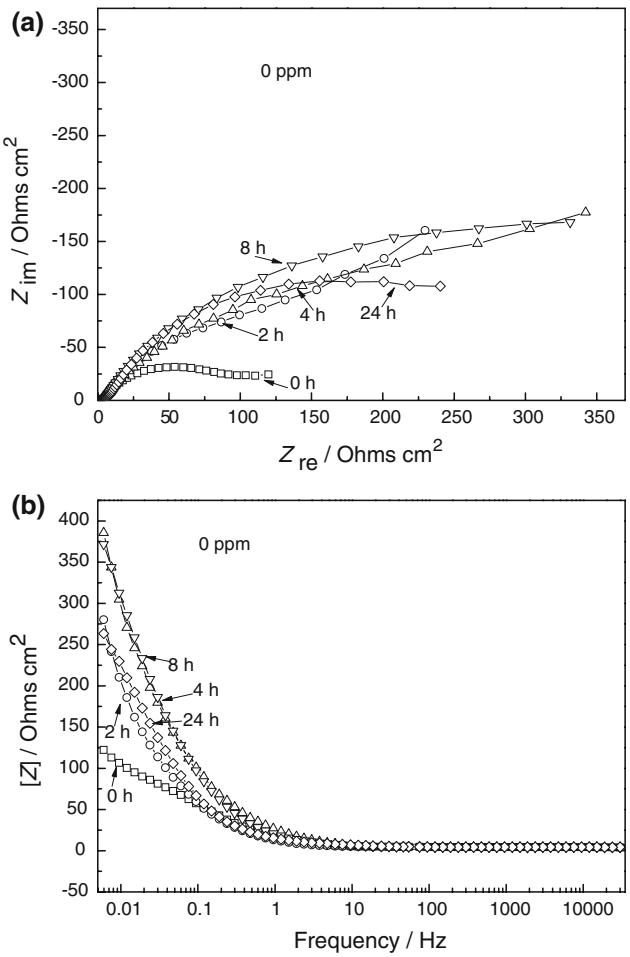


**Fig. 3** EIS data for $H_2S$-containing 3% NaCl solution without inhibitor in the **a** Nyquist and **b** Bode format

to the charge transfer from the metal to the solution, and a second semicircle at low frequencies, which, according to literature [9–11, 14] has been related to the formation of a porous film inhibitor. The second semicircle (the one at low frequencies) was not present at the beginning of the tests, indicating an absence of film inhibitor. The impedance modulus (Fig. 4b) increased with time up to 16 h, and afterward, it decreased. This behavior was similar with the addition of either 5 or 10 ppm of inhibitor. The Nyquist diagrams for the rest of the inhibitor concentrations showed only single, depressed, capacitive-like semicircles in the real axis, indicating that the corrosion process was under charge transfer control.

Figure 5 shows the change in impedance modulus with time for all the inhibitor concentrations. As seen, the lowest value for the modulus was obtained for the solution without inhibitor, while the highest value was obtained after adding 10 ppm inhibitor. This behavior was similar to that observed for $R_p$ (Fig. 2). Usually, when the Nyquist diagrams present a semicircle and the corrosion process is under charge transfer control, total impedance modulus is inversely proportional to the corrosion rate. Nevertheless, the relationship between corrosion rate and impedance modulus might not be so simple. Thus, taking this into account and according to Fig. 5, the highest impedance modulus was obtained with 10 ppm of inhibitor, and the lowest modulus, at least during the first few hours of testing, was obtained for solution without inhibitor as seen in the results for $R_p$ in Fig. 2. Once again, with exposure times longer than 8 h, the impedance modulus for the solution without inhibitor was slightly higher than that obtained when either 5 or 50 ppm of inhibitor was used. This trend was similar to the behavior observed for $R_p$ as shown in Fig. 2.

As an example of EN measurements, time records for both potential and current with 10 ppm of inhibitor at the beginning of the tests are plotted in Fig. 6. As seen, both signals show transients of high amplitude or intensity, and high frequency, indicative of a metal undergoing uniform corrosion. The combined effect of potential standard deviation, $\sigma_v$,, and current standard deviation, $\sigma_i$, results in noise resistance, $R_n$, (Eq. 1) which is inversely proportional to the corrosion rate, $I_{corr}$ as previously done with the $R_p$ values, Fig. 2, and the impedance modulus, Fig. 5. An estimation of the corrosion rate can be completed through the variation of $R_n$ with time for the different inhibitor concentrations, as can be seen in Fig. 7. This behavior is very similar to that observed in Figs. 2 and 5. As can be seen, initially $R_n$ was high, which corresponded to a low corrosion rate. Similarly, low $R_n$ observed toward the end of testing corresponded to an increase in corrosion rate. Generally speaking, the highest $R_n$ was obtained by adding 5 ppm of inhibitor during the first few hours of testing, and

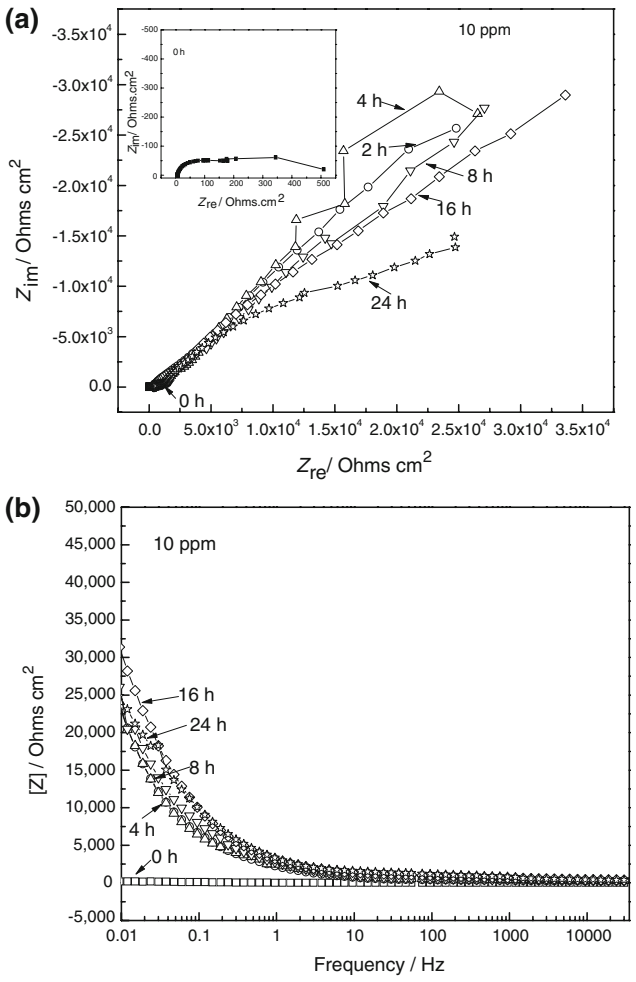


**Fig. 4** EIS data for the $H_2S$-containing 3% NaCl solution containing 10 ppm of hydroxyethyl imidazoline in the **a** Nyquist and **b** Bode format

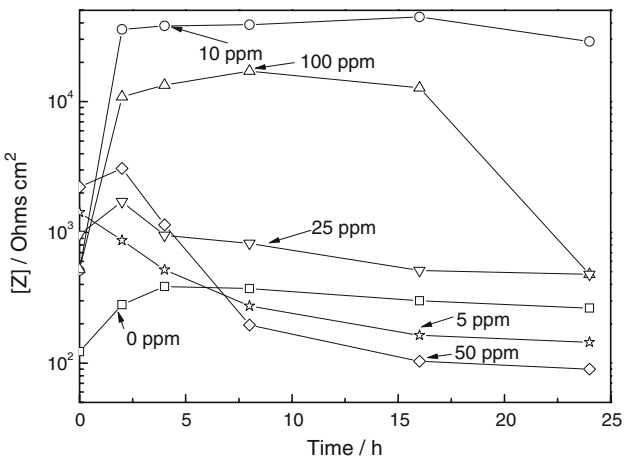


**Fig. 5** Effect of hydroxyethyl imidazoline concentration on the change of the impedance modulus over time

regardless of the inhibitor concentration, a decrease in corrosion rate was obtained. Nevertheless, this was not the case toward the end of testing as was observed for the $R_p$ results.

An index called "Localization index," LI, was calculated as:

$$\mathrm{LI} = \sigma_i / I_{\mathrm{rms}} \tag{4}$$

where $\sigma_i$ is the current standard deviation and $I_{\mathrm{rms}}$ is the current root mean square value [18]. LI has been correlated with the tendency toward localized or uniform corrosion. For LIs between 1 and 0.1, the alloy is highly susceptible to localized corrosion; for LI values between 0.01 and 0.001, the alloy is highly susceptible to uniform corrosion. Finally, for LI values between 0.1 and 0.01, the alloy is susceptible to a mixture of localized and uniform corrosion [18]. Figure 8 shows that at inhibitor doses lower than 50 ppm, the alloy is highly susceptible to localized corrosion, while at 50 or 100 ppm of inhibitor, it is susceptible to a mixture of uniform and localized corrosion.

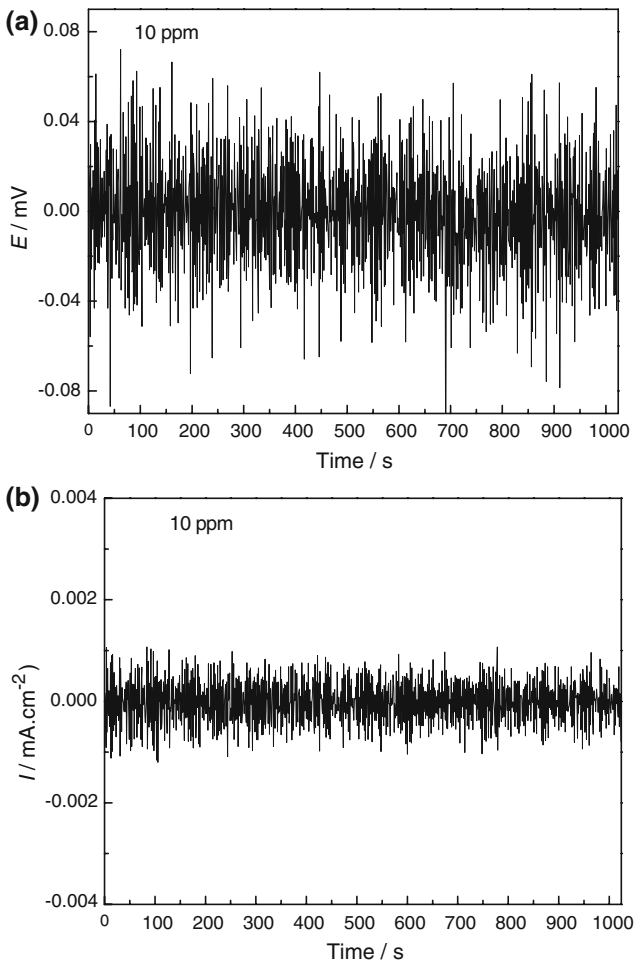


**Fig. 6** Time records for **a** potential noise and **b** current noise, obtained with 10 ppm of inhibitor

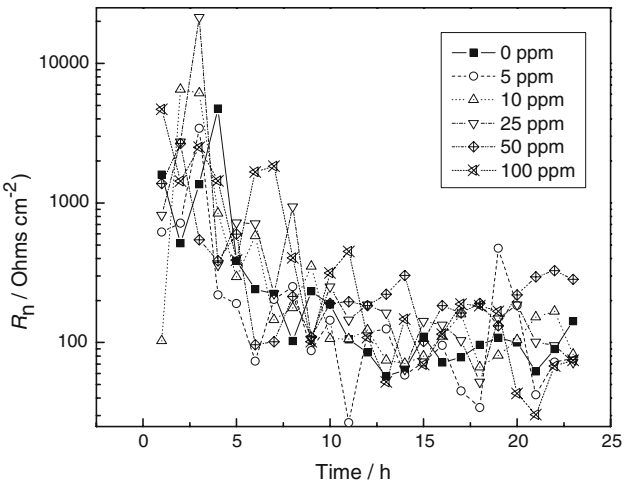


**Fig. 7** Effect of hydroxyethyl imidazoline concentration on the change in noise resistance value, $R_n$, over time in a $H_2S$-containing 3% NaCl solution

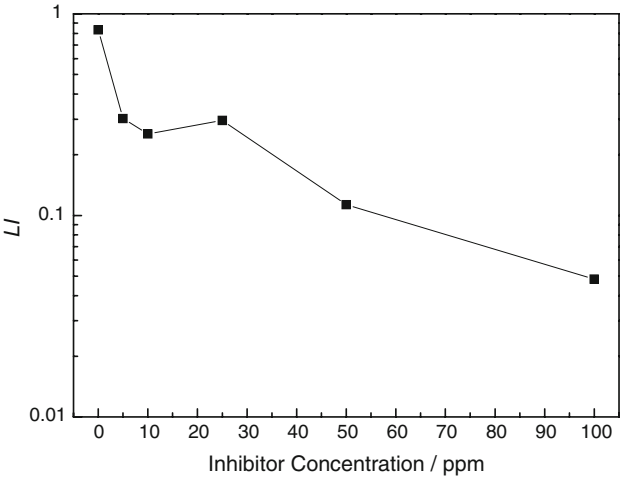


**Fig. 8** Effect of hydroxyethyl imidazoline concentration on the change in localization index value, LI, for a pipeline steel in a $H_2S$-containing 3% NaCl solution

Alternatively, the structure of the EN time records can be analyzed in the time domain and described by the Hurst exponent $H$ [19]. The development of fractal geometry by Mandelbrot [20] has provided mathematical tools for the analysis and characterization of the structure and scaling exponents of fractal time records. An EN time record is a "random" fractal, where the levels of detail are similar but not identical for the same statistical properties. The fractal dimension $D_f$ describes the structure of a fractal, e.g., the "roughness" of an EN time record and fractal geometry provides the explanation of the values for $D_f$, $H$, and $\beta$ that are observed for some of the EN time series parameters and noise spectra. Specifically, the fractional Brownian motion (fBm) Mandelbrot technique provides the connection between the structure of the EN time record and SDF

(characterized by $D_f$, $H$, and $\beta$) and microscopic behavior (oxidation reactions) responsible for corrosion. The fractal dimension $D_f$ is defined as

$$D_f = 2 - H = (5 - \beta)/2 \quad (5)$$

For example, the Hurst exponent $H$, which is formally related to $\beta$ reveals long-term time dependence in a time series and can be evaluated from oscillations occurring in the data. When the variation in the time record over a specific time interval (the lag time) is proportional to the lag time raised to the power $H$, the time series is said to be fractal. According to Hurst's rescaled range analysis based on his empirical law [19], we have

$$R/S = (\tau/2)^H \quad (6)$$

where $R$ represents the difference between the maximum and minimum of the variable, $S$ the standard deviation of the time series, $\tau$ the measured time, and $H$ the Hurst exponent. Parameter $H$ describes both the appearance of the time series ("roughness") and its characteristics: when $0.5 < H < 1$, oscillating signal or "persistence" can be seen; when $0 < H < 0.5$, a jagged signal "anti-persistence" is noted. When $H$ is equal to 0.5, the process is said to be completely random, statistically independent of each other. Hurst exponents, $H$, for both potential and current in and solution with and without 10 ppm of inhibitor are shown in Figs. 9 and 10, respectively. In both cases, it can be seen that $H$ was larger for solution containing 10 ppm of inhibitor and times shorter than approximately 8 h. After about 8 h, the Hurst exponents did not follow a constant trend. If Figs. 2 and 7 are checked, then it can be seen that after approximately 8 h, the efficiency of the hydroxyethyl imidazoline with 10 ppm started to decrease, and corrosion rates similar or higher than those found for uninhibited solutions were observed. This

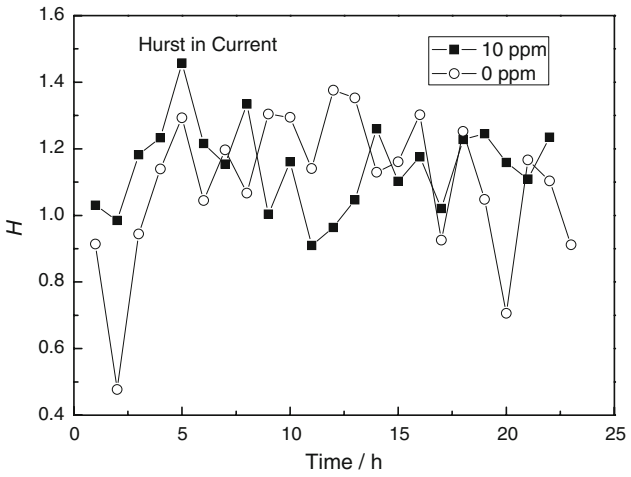


**Fig. 9** Change in Hurst exponent in current over time for steel in the solution containing 0 and 10 ppm of hydroxyethyl imidazoline

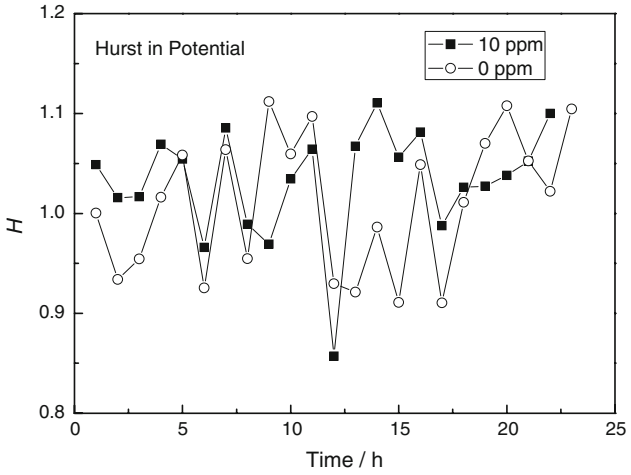


**Fig. 10** Change in the Hurst exponent in potential over time for steel in the solution containing 0 and 10 ppm of hydroxyethyl imidazoline

means that the time of residence, i.e., the time in which hydroxyethyl imidazoline remains on the metal surface is too short (around 8 h). This is due to the fact that we could not adjust any adsorption isotherm for this inhibitor. The best calculated efficiency for this inhibitor was used to obtain inhibitor coverage ($\Theta$), adsorbed over the metal surface. This is represented by the following equation:

$$\Theta = \%\mathrm{IE}/100 \quad (7)$$

where IE is inhibitor efficiency. A best fit was performed and compared using impedance and noise resistance with Langmuir, Temkin, Frumkin, and Flory–Huggins adsorption isotherm models. The adsorption isotherms show how adsorption varies with both activity and electrode charge. Langmuir isotherm model requires uniform activity over the surface for adsorption to take place with no interaction among adsorbed molecules. Frumkin and Temkin consider lateral interaction between adsorbed inhibitor molecules, while Flory–Huggins measures the previously adsorbed water molecules being displaced by an inhibitor molecule. None of these isotherms could be fitted to our data. This means that there is not strong adsorption of hydroxyethyl imidazoline on the steel surface. This could explain the short residence time of inhibitor on steel in $H_2S$-containing 3% NaCl solution.

The corrosion resistance of a protective inhibitor film is often related to its susceptibility toward local breakdown and pits initiation. It has been demonstrated that pit growth occurs in two consecutive stages which is characterized by metastable growth in its early stage, followed by stable growth [21]. Metastable pits cause no great damage to the material because their diameters are typically on the order of a few micrometers. Moreover, the early development of stable pits is identical to that of metastable pits [22], and the probability of stable pitting is directly linked to the

occurrence and intensity of metastable pitting. Thus, in the absence of inhibitor or concentrations lower than 50 ppm as is evident in Fig. 8, the probability of stable pitting was higher for low inhibitor concentrations due to the fact that its LI values were higher than the ones obtained with inhibitor concentrations higher than 50 ppm. This is common with inhibitors that they are used in concentrations which do not cover the entire surface and, therefore, some uncovered sites remain in which aggressive ions such as $Cl^-$ or $S^{2-}$ can attack the metal surface. Once critical concentration has been reached, in this case around 50 ppm, in such a way that the whole metal surface is covered by the inhibitor, the number of active sites is lowered and, thus, the probability for localized attack. This increases the pitting potential, Fig. 10. This was shown by the Nyquist plots at 10 ppm, Fig. 4, which showed the presence of one semicircle at high frequencies, related to the charge transfer from the metal to the solution, and a second semicircle at low frequencies, related to the presence of a porous inhibitor layer. This behavior was found only at 5 and 10 ppm of inhibitor.

## 4 Conclusions

The effect of hydroxyethyl imidazoline on the $H_2S$ corrosion inhibition of a pipeline steel has been studied by LPR, EIS, and EN measurements. All techniques showed that highest inhibitor efficiency was reached by adding between 5 and 10 ppm of inhibitor. However, at doses lower than 5 ppm, Nyquist diagrams showed that the inhibitor formed a layer which made the steel highly susceptible to localized corrosion. For doses higher than 10 ppm, the presence of an inhibitor layer was not evident, and the steel was susceptible to a mixture of uniform and localized corrosion. Thus, EN measurements can be used not only to predict corrosion types, i.e., localized or uniform, but also corrosion rates. Hurst exponent calculations showed that this was higher in presence of hydroxyethyl imidazoline only for short times, indicating the short residence time of this inhibitor. The results could not be fitted to any adsorption isotherm, which means that there was an absence of strong interaction between the inhibitor and the metal surface.

## References


1. Kermani MB, Morshed A (2003) Corrosion 59:659
2. Smith SN (1993) A proposed mechanism for corrosion in slightly sour oil and gas production. In: Proceedings of the 12th international corrosion congress held in September 19–23, 1993, NACE International, Houston, TX
3. Foroulis ZA (1993) Corros Prev Control 40:84
4. Jovancicevic V, Ramachandran S, Prince P (1999) Corrosion 55:449
5. Ramachandran S, Jovancicevic V (1999) Corrosion 55:259
6. Xueyuan Z (2001) Corros Sci 43:1417
7. Bentiss F, Lagrenee M, Traisnel M, Hornez JC (1999) Corros Sci 41:789
8. Ramachandran S, Tsai BL, Blanco M, Chen H, Tang Y, Goddard WA (1996) Langmuir 12:6419
9. Wang D, Li S, Ying M, Wang M, Xiao Z, Chen Z (1999) Corros Sci 41:1911
10. Popova A, Raicheva S, Sokolova E, Christov M (1996) Langmuir 12:2083
11. Nykos L, Pajlossy T (1985) Electrochim Acta 30:1533
12. Garcia-Ochoa E, Genesca J (2004) Surf Coat Technol 184:322
13. Samiento-Bustos E, González Rodriguez JG, Uruchurtu J, Dominguez-Patiño G, Salinas-Bravo VM (2008) Corros Sci 50:2296
14. Tan YJ, Bailey S, Kinsella B (1996) Corros Sci 38:1681
15. NACE MR0175-2003 (2003) Petroleum and natural gas industries—materials for use in $H_2S$-containing environments in oil and gas production. National Association of Corrosion Engineers
16. Tewart PH, Campbell AB (1979) Can J Chem 57:188
17. Meyer FH, Riggs OL, McGlasson RL, Sudbury JD (1958) Corrosion 14:69
18. AL-Zanki IA, Gill JS, Dawson JL (1986) Mater Sci Forum 8:463
19. Mandelbrot BB (1991) The fractal geometry of nature. W. H. Freeman & Co., New York
20. Feder J (1989) Fractals. Plenum Press, New York
21. Bard AJ, Stratman M (2003) Encyclopedia of electrochemistry, vol 4: corrosion and oxide films. Wiley–VCH, p 435
22. Badawy W, Al-Kharafi FM, El-Ezab AS (1999) Corros Sci 41:709